Available online at www.sciencedirect.com

ScienceDirect

Procedia Engineering 188 (2017) 209 – 216

Procedia Engineering

www.elsevier.com/locate/procedia

6th Asia Pacific Workshop on Structural Health Monitoring, 6th APWSHM

Identification of Zero Effect State in Corroded RCC Structures Using Guided Waves and Embedded Piezoelectric Wafer Transducers (PWT)

Rajeshwara C.S.[a,b,c,*], Sauvik Banerjee[b] , Ye Lu[c]

[a]*IITB-Monash Research Academy, Indian Institute of Technology Bombay, Powai, Mumbai 400076, India*
[b]*Department of Civil Engineering, Indian Institute of Technology Bombay, Powai, Mumbai 400076, India*
[c]*Department of Civil Engineering, Monash University, Clayton, VIC 3800, Australia*

Abstract

Reinforced cement concrete (RCC) structures are prone to damages such as corrosion of reinforcement, surface cracking, debonding and the like. The corrosion process results in two effects, namely, reduction in the diameter of rebar and debonding at the steel/concrete interface. Several researchers have worked to establish a correlation between intrinsic damage features and guide wave signal characteristics. However, the work till date is focused mainly on identifying the individual damage phenomenon, and few researchers have attempted to correlate the combined effect of these damage parameters. Therefore, it is an impending task to study the combined influence of corrosion and debonding on wave characteristics and to establish methods to distinguish and correctly quantify the damage level. A three-dimensional finite element model of a RCC beam is developed in the Abaqus software by using an explicit method in order to study wave propagation in an RCC beam after including the two effects of corrosion. The implicit and explicit models are co-executed using standard-explicit co-simulation. It is observed that the reduction in diameter would result in the diminishing of the guided wave amplitude, whereas debonding results in an increase in the guided wave amplitude. It is found that these two complimentary effects on wave features result in a signal that has the same wave features as undamaged rebar that is surrounded by concrete, which could be termed as the zero effect state.

Peer-review under responsibility of the organizing committee of the 6th APWSHM

* Corresponding author. Tel.: +91-22-2576-4343; fax: +91-22-2576 7302
E-mail address: rcsriramadasu@gmail.com rajeshwara.sriramadasu@monash.edu

Peer-review under responsibility of the organizing committee of the 6th APWSHM
doi:10.1016/j.proeng.2017.04.476

*Keywords:*Corrosion; Concealed damage; Concrete; Debonding; Guided waves

1. Introduction

Concrete is a widely used material in the infrastructure industry due to its easy availability, high compressive strength-to-density ratio, ability to form into the required shape, and its lower cost when compared to its metal counterparts. In order to increase the tensile strength of concrete, reinforcing bars (rebars) are embedded in it. Reinforced concrete structures are prone to damages such as surface cracking of concrete; corrosion of steel; debonding of steel due to various factors such as weathering, chemical attack, overloading, aging, and the like. Concrete acts as a natural protector against the corrosion of rebars by serving as an alkaline medium. However, ingress of chloride ions over extended periods of time neutralizes the cathodic protection, and the reinforcing bars corrode. In this process, the pore solution serves as electrolyte, and the rebar acts as a mixed electrode, that is, a part of the bar acts as a cathode, whereas another part acts as an anode, leading to pitting corrosion[1]. Eventually, rust begins to form, which can lead to another kind of damage, namely, debonding of steel and concrete at the interface. Hence, prior diagnosis of apparently healthy concrete would help in taking preventive action, which would reduce the maintenance cost and improve the safety and reliability of Reinforced cement concrete (RCC) structures.

Several researchers have studied corrosion by attaching ultrasonic transducers to the ends of the rebar [2][3][4]. However, such a method is not field deployable because the ends of rebars may not be available for the attaching of the transducers. Embedded smart aggregates have been used as transducers to monitor the strength of early age concrete, detect impact location [5], and monitor cracks in concrete [6]. An embedded smart aggregate can capture the early ingress of chloride ions and, therefore, can detect the onset of the corrosion process. However, the passive film that protects the embedded sensor may get damaged during the corrosion process due to which the smart aggregate becomes unusable [7]. Due to their durability, sensors that are bonded on the surface of the rebar prove to be more effective than smart aggregates in monitoring the corrosion. Piezoelectric wafer transducers (PWT) sensors, which can be attached to the surface of the rebar, promise to be better a alternative.

Researchers have tried to correlate the level of corrosion in rebars in RCC beams by using differential time of flight measurements [8][9]. In a typical reinforced concrete structure, more than one rebar is embedded in concrete. In previous studies by researchers[10], it has been observed that the presence of damage in a nearby bar affects the received signal of the rebar under examination; therefore, locating the damage becomes more complicated. Recently advanced techniques such as principal component analysis[11], genetic algorithms, neural networks [12], simulated annealing, and particle swarm optimization[13] have been applied in damage diagnosis.

Although various kinds of damages have been extensively studied individually, the combined effect of these damages has not been studied much. Based on the studies on damages of corrosion and debonding it can be established that these two effects have complementary effects on wave characteristics [2][14]. In the present study, it is shown that the combination of a reduction in the diameter of rebar due to corrosion and separation of rebars and concrete due to debonding may conceal the damage. Hence, further studies are required to investigate the influence of corrosion on wave characteristics in reinforced concrete structures, and to establish methods to distinguish and correctly quantify the level of damage. To meet this objective, a three-dimensional finite element model of an RCC beam is developed using an explicit method in Abaqus software in order to study guided wave propagation that is generated by embedded PWT. Corrosion in rebar is simulated by reducing the diameter of the rebar, and debonding is simulated by untying the concrete and the rebar. The dynamic-implicit method is used to simulate piezoelectric material. The implicit and explicit models are co-executed using standard-explicit co-simulation. The two complementary effects of corrosion and disbond on wave features, which results in a zero effect state, are studied in detail.

2. Guided wave propagation in reinforced concrete structures

The philosophy of guided waves has originated from the work of Lord Rayleigh[15]. It was followed by Horace Lamb's work in which Horace Lamb has established theoretical fundamentals of waves that can propagate in plate-like structures with free surfaces [16]. These waves are called Lamb waves.

Analogous to plate structures, when an elastic wave propagates through cylindrical elements, the surfaces of which act as waveguides, various modes are generated. The torsional mode is analogous to the shear horizontal mode in the plate structure. Similarly, the longitudinal mode corresponds to the symmetric mode and the flexural mode corresponds to the antisymmetric mode.

The governing equation for wave propagation is given by (1)

$$(\lambda+\mu)\nabla\nabla.\mathbf{U}+\mu\nabla^2\mathbf{U}+\rho f=\rho\ddot{\mathbf{U}} \tag{1}$$

where **U** is the displacement vector, f is the body force vector, ρ is the density, and λ and μ are Lame parameters.

The solution to the governing equation that uses the Gazis method, which is mentioned above, will be of the form presented in equation (2)

$$u_r = A_r(r)\cos(m\theta)e^{i(kz-\omega t)} \tag{2a}$$

$$u_\theta = A_\theta(r)\sin(m\theta)e^{i(kz-\omega t)} \tag{2b}$$

$$u_z = A_z(r)\cos(m\theta)e^{i(kz-\omega t)} \tag{2c}$$

The two sets of equations above, when solved for the traction-free boundary condition on the cylindrical surface gives a system of homogeneous equations. The solution to these equations leads to dispersion curves. A typical dispersion curve for a rod of 20 mm is shown in Figure 1. A detailed study on wave propagation in cylindrical waveguides can be found in Ref. [17].

3. Numerical modeling

Wave propagation in reinforced concrete is complex due to the composite nature of concrete. In order to simplify the analysis, concrete is assumed to be isotropic and elastic. The presence of two different materials, namely, concrete and reinforcement steel makes it impossible to calculate the wave characteristics analytically; therefore, numerical modeling is adopted. For the current study, commercial finite element software, Abaqus/CAE 6.13, is used. The inbuilt ability of the software to simulate electrical excitation and mechanical wave propagation simultaneously is utilized in this study. Explicit code is used to model the reinforced concrete, and implicit code is used to model the PWT. These two codes are executed simultaneously using standard-explicit co-simulation, which is available in the software[18].

For the current study, the electro-mechanical properties that correspond to SP-5H PWTs are used, as presented in Ref. [19], and the properties of concrete and steel are listed in Table-1. A concrete beam that has the dimensions, 150 mm x 100 mm x 500 mm, is embedded with a rebar of a length of 1.5m. PWTs are attached to the surface of rebars at each end. A schematic representation of the model is shown in Figure 2.

A narrowband five-cycle hanning pulse is used as input for wave generation at a frequency of 100 kHz. The response of the structure is show in Figure 3(a). It is analyzed by using Gabor Wavelet, the wavelet coefficients of which are plotted in Figure 3(b). It is observed that the given excitation results in two wave modes, and these are recognized as the longitudinal mode L(0,1) and the flexural mode F(1,1); the flexural mode has dominant energy.

Dispersion curves for a rebar with a diameter of 20 mm are plotted using the group velocity that is obtained from numerical results. These dispersion curves were verified by conducting experiments on bare rebar by changing the excitation frequency. The results are shown in Figure 1.

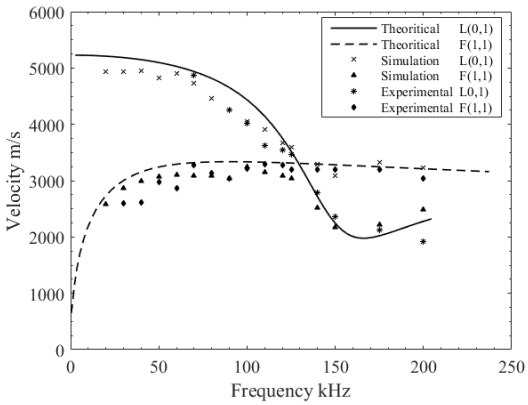

Figure 1 Dispersion curves for a rod that is 20 mm in diameter, showing longitudinal and flexural modes.

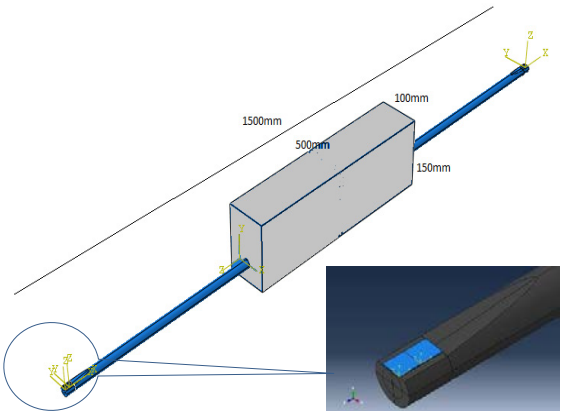

Figure 2 Schematic diagram of the reinforced concrete beam that was used in study of corrosion and de-bonding.

Table 1 Mechanical Properties of materials

Material	Density (kg/m3)	Poisson ratio	Young's Modulus (GPa)
Concrete	2500	0.15	25
Steel	7850	0.30	200

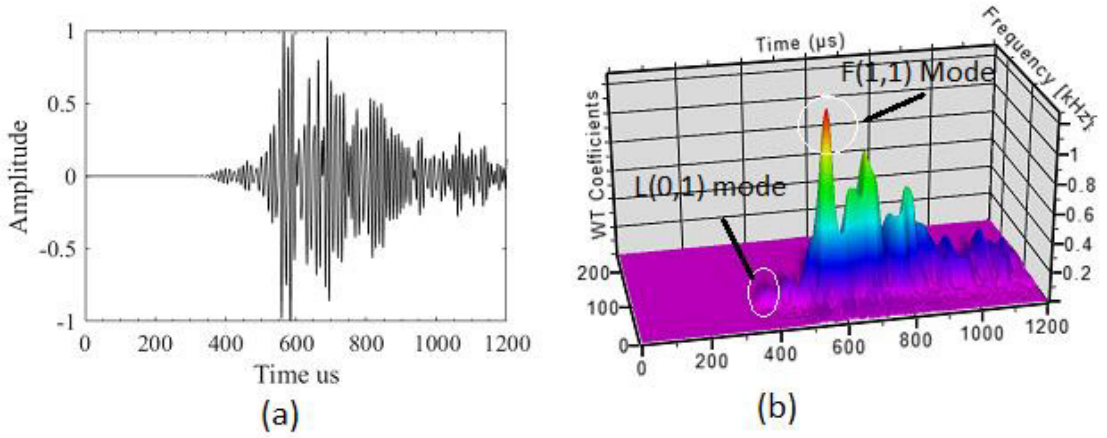

Figure 3 Response of an undamaged structure at 100 kHz excitation frequency (a) Time History (b) 3D plot of signal using Gabor wavelet

4. Results and discussion

4.1. Corrosion of rebars in concrete

Corrosion in rebars is induced by reducing the diameter of the rebar. The contact between the rust that is formed during corrosion and the intact rebar is maintained by tying them. A parametric study is carried out by varying the extent of the corrosion in two different ways, namely, by reducing the diameter of the rebar for a specified length and by increasing the length of the corroded bar.

In Figure 4 and Figure 5, the time histories and the energy envelopes of the intact specimen and a corroded specimen are compared. The corrosion is simulated at the center of the rebar by reducing the diameter of the rebar to 16mm from 20mm over a length of 200mm. A decrease is observed in the wave amplitudes of the L(0, 1) mode and the F(1, 1) mode with the increase in the corrosion level, as shown in Figures 6 and 7, respectively. Also, the speed of the wave is observed to be lower than that of an undamaged rebar. This phenomenon confirms that as the bar gets corroded, more energy is leaked into the surroundings and, hence, the observed energy is considerably lower than that of an intact specimen. Results of the parametric study show a quadratic decreasing trend in the wave amplitudes of the two fundamental modes.

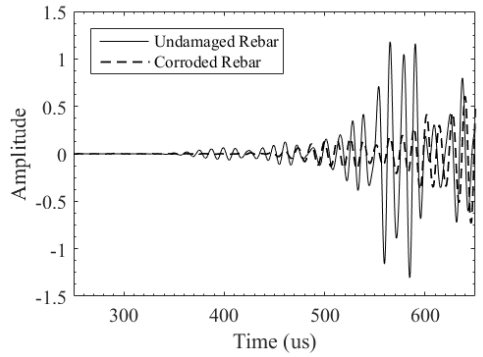

Figure 4 Comparison of signals received in an undamaged specimen and a corroded specimen

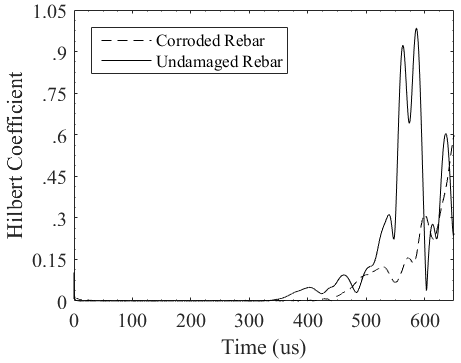

Figure 5 Energy envelope of an undamaged specimen and a specimen subjected to corrosion

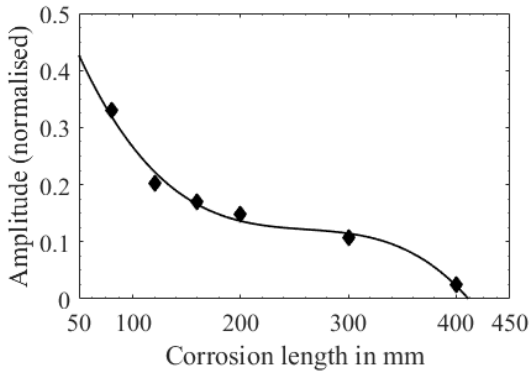

Figure 6 Variation of amplitude of L(0, 1) mode with corrosion along the length of the rebar.

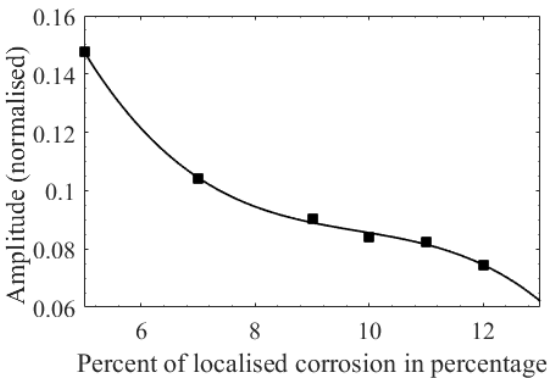

Figure 7 Variation of amplitude of F(1, 1) mode with pitting type of corrosion in the rebar.

4.2. Debonding of rebars and steel

Debonding is simulated by untying the rebar and the concrete at the interface. The variations in the wave amplitude and the group velocity with the debond length are plotted in Figure 8 and Figure 9. It is observed that the amplitude of the received signal increases exponentially with the increase in the debond length (Figure 8). This can be attributed to the fact that with an increase in the debond length, the loss of energy to the surrounding concrete medium is less, and the wave energy is more focused in the rebar. The observed exponential trend in the parametric study conforms to the study by Wu et al.[20]. For the debonded specimen, the group velocity of the L(0, 1) mode is faster than that of an undamaged specimen. Also, as shown in Figure 9, the wave velocity rises with the increase in the debond length and finally attains the wave speed in a bare rebar.

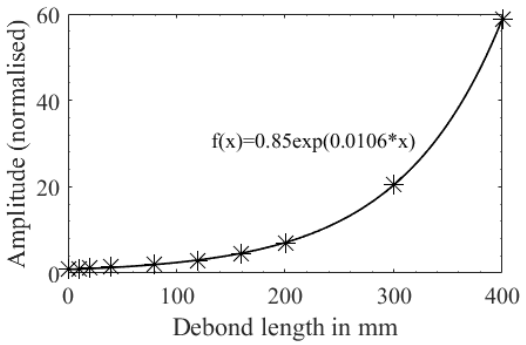

Figure 8 Variation of amplitude of L(0, 1) mode with increase in debond between steel and concrete

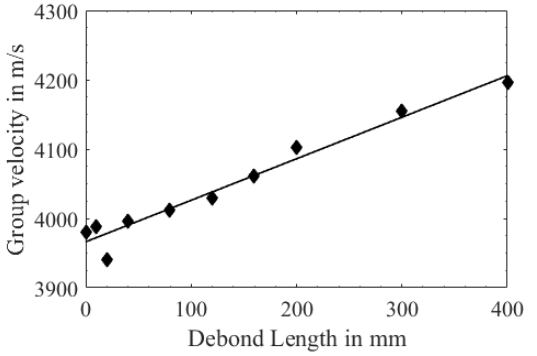

Figure 9 Variation of velocity of L(0, 1) mode with increase in debond between steel and concrete

4.3. Combined effect of debonding and corrosion

In a typical reinforced concrete structure, the damages of debonding and corrosion occur simultaneously. A rebar that is subjected to prolonged corrosion will develop rust. As this rust separates from the host rebar, it leads to debonding. From the discussion in the preceding sections, it is observed that these two kinds of damages have complementary effects on wave characteristics. Hence, it is an impending task to study these two damages together. An undamaged concrete beam, which is subjected to the corrosive environment is considered in the study. With the onset of corrosion, the diameter of the intact rebar reduces gradually, and rust develops along the perimeter of the rebar. As the volume of the corrosion product becomes bulkier, it leads to the scaling of rust, resulting in separation between the layers of the intact rebar and rust, which can be termed as debond [21]. Based on this premise, the L(0, 1) mode was chosen and numerical investigations were carried out for various cases of damage to find the zero effect state.

Curve “0” in Figure 10 shows the energy envelope of response that was obtained in an undamaged rebar. Corrosion damage that is 80 mm wide is simulated at the center of the rebar. It is observed from curve “1” that the amplitude and the velocity of the signal are reduced with the corrosion of the rebar. On the other hand, from curve “2” a sudden jump in amplitude and velocity is observed when a disbond is initiated between the rebar and the concrete. As the

rebar is allowed to corrode further (Curves 3, 4 and 5) along with a uniform reduction in the diameter, the amplitude of the signal gradually approaches that of the undamaged specimen.

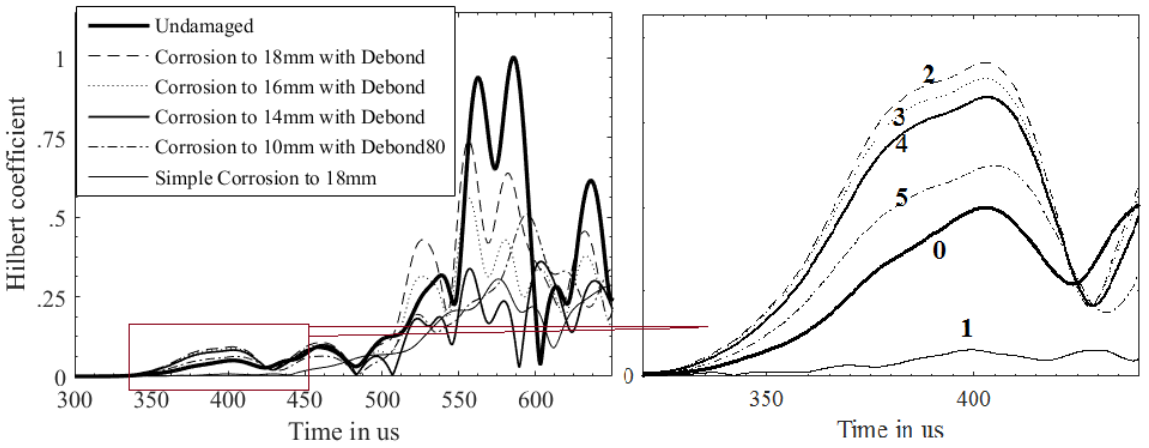

Figure 10 Comparison of energy envelops for various damage scenarios, in order to identify the zero state effect for damage that is located at the centre of the rebar.

An important inference can be drawn from Figure 10: With the onset of disbond in the rebar that is subjected to corrosion, due to separation of the rust, a sudden rise in amplitude and velocity of L(0, 1) mode can be observed. As the corrosion progresses from this stage, the wave characteristics gradually approach that of an undamaged stage. In fact, such a zero state effect is independent of the initial damage. In a similar phenomenon, a damaged rebar that shows wave characteristics that are equivalent to an undamaged rebar can, therefore, be expected from a rebar that has initial disbond and is subjected to corrosion at a later stage.

The study is repeated with different lengths of damage and it is found that the zero effect state can be located for damage of any size. The possibility of a zero effect state for varying damage sizes makes it impossible to identify an abrupt change in the wave characteristics due to the onset of debond or corrosion. Further study is required to ascertain the observed phenomenon experimentally and also to establish methods to identify and distinguish the damages.

5. Conclusions

In this study, two different kinds of defects, namely, corrosion and debonding, which occur in RCC, are numerically investigated using guided waves that are generated using PWT that is attached on the surface of the rebar. It is observed that these two damages have complementary effects on wave characteristics. It is demonstrated that co-occurrence of more than one damage may lead to a zero effect state and, hence, a possibility of concealed damage. It is also observed that there can be more than one zero effect state in the corrosion process, which necessitates the development of techniques to study various kind of damages simultaneously.

Acknowledgements

The authors acknowledge the support of IITB-Monash Research Academy for the grant provided under the project number IMURA-383.

References

[1] S. Ahmad, "Reinforcement corrosion in concrete structures, its monitoring and service life prediction–a review," *Cem. Concr. Compos.*, vol. 25, no. 4, pp. 459–471, 2003.

[2] T. H. Miller, T. Kundu, J. Huang, and J. Y. Grill, "A New Guided Wave Based Technique for Corrosion Monitoring in Reinforced Concrete," *Struct. Heal. Monit.*, 2012.

[3] B. L. Ervin and H. Reis, "Longitudinal guided waves for monitoring corrosion in reinforced mortar," *Meas. Sci. Technol.*, vol. 19, no. 5, p. 55702, May 2008.

[4] S. Sharma and A. Mukherjee, "Nondestructive Evaluation of Corrosion in Varying Environments Using Guided Waves," *Res. Nondestruct. Eval.*, vol. 24, no. 2, pp. 63–88, 2013.

[5] G. Song, H. Gu, and Y.-L. Mo, "Smart aggregates: multi-functional sensors for concrete structures—a tutorial and a review," *Smart Mater. Struct.*, vol. 17, no. 3, p. 033001, Jun. 2008.

[6] C. Dumoulin, G. Karaiskos, and A. Deraemaeker, "Monitoring of crack propagation in reinforced concrete beams using embedded piezoelectric transducers," *VIII Int. Conf. Fract. Mech. Concr. Concr. Struct.*, pp. 1717–1725, 2013.

[7] V. Talakokula and S. Bhalla, "Reinforcement corrosion assessment capability of surface bonded and embedded piezo sensors for reinforced concrete structures," *J. Intell. Mater. Syst. Struct.*, vol. 26, no. 17, pp. 2304–2313, 2014.

[8] U. Amjad, S. K. Yadav, and T. Kundu, "Detection and quantification of diameter reduction due to corrosion in reinforcing steel bars," *Struct. Heal. Monit.*, vol. 14, no. 5, pp. 532–543, 2015.

[9] U. Amjad, S. K. Yadav, and T. Kundu, "Detection and quantification of diameter reduction due to corrosion in reinforcing steel bars," *Struct. Heal. Monit.*, 2015.

[10] S. Mustapha, Y. Lu, J. Li, and L. Ye, "Damage detection in rebar-reinforced concrete beams based on time reversal of guided waves," *Struct. Heal. Monit.*, vol. 13, no. 4, pp. 347–358, 2014.

[11] Y. Lu, J. Li, L. Ye, and D. Wang, "Guided waves for damage detection in rebar-reinforced concrete beams," *Constr. Build. Mater.*, vol. 47, pp. 370–378, 2013.

[12] J. Min, S. Park, C.-B. Yun, C.-G. Lee, and C. Lee, "Impedance-based structural health monitoring incorporating neural network technique for identification of damage type and severity," *Eng. Struct.*, vol. 39, pp. 210–220, 2012.

[13] R. Sun, E. Sevillano, and R. Perera, "Debonding detection of FRP strengthened concrete beams by using impedance measurements and an ensemble PSO adaptive spectral model," *Compos. Struct.*, vol. 125, pp. 374–387, 2015.

[14] T. Miller, C. J. Hauser, and T. Kundu, "Nondestructive Inspection of Corrosion and Delamination at the Concrete-Steel Reinforcement Interface," *Nondestruct. Eval.*, vol. 2002, pp. 121–128, 2002.

[15] Lord Rayleigh, "On waves propagating along the plane surface of an elastic solid," *Proc. London Math. Soc.*, vol. 7, no. 1, pp. 4–11, 1885.

[16] H. Lamb, "On waves in an elastic plate," *Proc. R. Soc. London. Ser. A, Contain. Pap. a Math. Phys. character*, pp. 114–128, 1917.

[17] J. L. Rose, *Ultrasonic Waves in Solid Media*. Cambridge university press, 2014.

[18] S. Sikdar and S. Banerjee, "Identification of disbond and high density core region in a honeycomb composite sandwich structure using ultrasonic guided waves," *Compos. Struct.*, vol. 152, pp. 568–578, 2016.

[19] S. Sikdar, S. Banerjee, and G. Ashish, "Ultrasonic guided wave propagation and disbond identification in a honeycomb composite sandwich structure using bonded piezoelectric wafer transducers," *J. Intell. Mater. Syst. Struct.*, pp. 1–13, 2015.

[20] F. Wu, H.-L. Chan, and F.-K. Chang, "Ultrasonic guided wave active sensing for monitoring of split failures in reinforced concrete," *Struct. Heal. Monit.*, p. 1475921715591876–, 2015.

[21] A. A. Almusallam, A. S. Al-Gahtani, A. R. Aziz, and Rasheeduzzafar, "Effect of reinforcement corrosion on bond strength," *Constr. Build. Mater.*, vol. 10, no. 2, pp. 123–129, Mar. 1996.